

MSc Computational Science  
joint programme UvA/VU



# MODELLING DIFFUSIVE SIGNALLING IN *ASPERGILLUS* SPP. GERMINATION INHIBITION



INTERMEDIATE PRESENTATION - MAY

Presented by Boyan Mihaylov

May 2, 2025

Supervisor: Prof. dr. Han Wösten, Utrecht University

Examiner: Dr. Jaap Kaandorp, University of Amsterdam

# OUTLINE



## 1 Single-spore experiments: revision

Introduction

Revision of diffusivities/permeabilities

Barrier scenarios

Table of permeabilities

Single-spore release scenarios

Cell wall adsorption model

## 2 Spore cluster experiments: revision

Introduction

Homogeneous vs. cell-wall-bound inhibitor

Extreme cases

Functional relationship

## 3 From a deterministic to a statistical model

Deriving the germination probability

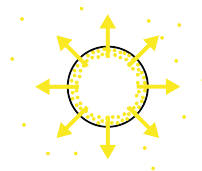
Parameter estimation

# SINGLE-SPORE EXPERIMENTS: REVISION



## Introduction

- » The goal is to test if **interface permeability theory** (spore as a "leaky balloon") can be used to estimate meaningful properties of a non-replenishable germination inhibitor released by the spore.



# SINGLE-SPORE EXPERIMENTS: REVISION



## Revision of diffusivities/permeabilities

- » A lower limit (200 nm) and an upper limit (400 nm) of the cell wall thickness are considered, of which 10 nm is the rodlet-melanin layer, the rest considered mainly polysaccharides (membrane considered separately):

1-octen-3-ol	$D$	$P_{\text{eff}}$
water (400 nm)	$6.9016 \times 10^{-6} \text{ cm}^2 \text{ s}^{-1}$	$0.172\,54 \text{ cm s}^{-1}$
agarose-like layer (190 nm)	$6.9016 \times 10^{-6} \text{ cm}^2 \text{ s}^{-1}$	$0.363\,24 \text{ cm s}^{-1}$
agarose-like layer (390 nm)	$6.9016 \times 10^{-6} \text{ cm}^2 \text{ s}^{-1}$	$0.176\,96 \text{ cm s}^{-1}$
cellulose-like layer (190 nm)	$1.9555 \times 10^{-7} \text{ cm}^2 \text{ s}^{-1}$	$0.010\,292\,1 \text{ cm s}^{-1}$
cellulose-like layer (390 nm)	$1.9555 \times 10^{-7} \text{ cm}^2 \text{ s}^{-1}$	$0.005\,014\,1 \text{ cm s}^{-1}$
lipid bilayer membrane (3.8 nm)	$1.086 \times 10^{-13} \text{ cm}^2 \text{ s}^{-1}$	$9.04 \times 10^{-5} \text{ cm s}^{-1}$
hydrophobin layer (10 nm)	$1.086 \times 10^{-13} \text{ cm}^2 \text{ s}^{-1}$	$3.43 \times 10^{-5} \text{ cm s}^{-1}$

Table: Diffusion coefficient ( $D$ ) and effective permeability ( $P_{\text{eff}}$ ) of 1-octen-3-ol through various media.

# SINGLE-SPORE EXPERIMENTS: REVISION



## Revision of diffusivities/permeabilities

- » A lower limit (200 nm) and an upper limit (400 nm) of the cell wall thickness are considered, of which 10 nm is the rodlet-melanin layer, the rest considered mainly polysaccharides (membrane considered separately):

heat-labile peptide	$D$	$P_{\text{eff}}$
water (400 nm)	$4.548\,55 \times 10^{-7} \text{ cm}^2 \text{ s}^{-1}$	$0.011\,37 \text{ cm s}^{-1}$
agarose-like layer (190 nm)	$4.548\,55 \times 10^{-7} \text{ cm}^2 \text{ s}^{-1}$	$0.023\,939\,7 \text{ cm s}^{-1}$
agarose-like layer (390 nm)	$4.548\,55 \times 10^{-7} \text{ cm}^2 \text{ s}^{-1}$	$0.011\,662\,9 \text{ cm s}^{-1}$
cellulose-like layer (190 nm)	$1.29 \times 10^{-8} \text{ cm}^2 \text{ s}^{-1}$	$6.789 \times 10^{-4} \text{ cm s}^{-1}$
cellulose-like layer (390 nm)	$1.29 \times 10^{-8} \text{ cm}^2 \text{ s}^{-1}$	$3.3 \times 10^{-4} \text{ cm s}^{-1}$
lipid bilayer membrane (3.8 nm)	N/A	N/A
hydrophobin layer (10 nm)	N/A	N/A

Table: Diffusion coefficient ( $D$ ) and effective permeability ( $P_{\text{eff}}$ ) of the heat-labile peptide through various media.

# SINGLE-SPORE EXPERIMENTS: REVISION



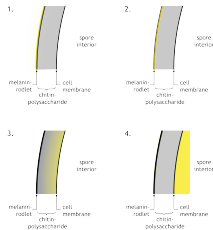
## Barrier scenarios

- » When combining layers with different permeabilities, the net permeation constant  $P_{\text{eff}}$  can be computed via the formula [1]

$$\frac{1}{P_{\text{eff}}} = \frac{1}{P_1} + \frac{1}{P_2} + \dots + \frac{1}{P_n}, \quad (1)$$

where  $P_i$ ,  $i = 1, 2, \dots, n$  are the permeabilities of the separate layers.

- » Some possible permeation-defining configurations are:
1. an inhibitor source and receiver expressed in the **outermost layer** of the cell wall, virtually unobstructed by any layers, only limited by diffusion in water;
  2. an inhibitor source and receiver **embedded between the inner and outer cell wall layers**, obstructed only by the hydrophobin-melanin layer;
  3. an inhibitor source and receiver embedded **deep in the inner cell wall layer**, obstructed by polysaccharide network and the hydrophobin-melanin layer;
  4. an inhibitor source and receiver **inside the spore interior**, obstructed by the cell membrane and the entire cell wall.



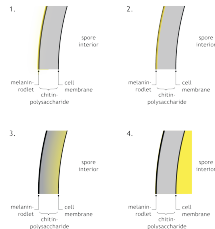
# SINGLE-SPORE EXPERIMENTS: REVISION



## Barrier scenarios

» Disregarding the effect of unstirred water around the spore, these scenarios can be translated into permeabilities as follows:

1.  $P_{\text{eff}} \approx \infty$ ,
2.  $P_{\text{eff}} \approx P_{\text{hp}}$ ,
3.  $P_{\text{eff}} = \left( \frac{1}{P_{\text{hp}}} + \frac{1}{P_{\text{agar}}} \right)^{-1}$  or  $P_{\text{eff}} = \left( \frac{1}{P_{\text{hp}}} + \frac{1}{P_{\text{cel}}} \right)^{-1}$ ,
4.  $P_{\text{eff}} = \left( \frac{1}{P_{\text{hp}}} + \frac{1}{P_{\text{agar}}} + \frac{1}{P_{\text{lb}}} \right)^{-1}$  or  $P_{\text{eff}} = \left( \frac{1}{P_{\text{hp}}} + \frac{1}{P_{\text{cel}}} + \frac{1}{P_{\text{lb}}} \right)^{-1}$ .



# SINGLE-SPORE EXPERIMENTS: REVISION



## Table of permeabilities

- » As the outermost layer is impermeable for large proteins, the permeation of a heat-labile peptide can only be considered during the onset of swelling, i.e. when the rodlet layer begins losing its integrity.

Barrier type	$P_{\text{eff}}(1\text{-octen-3-ol})$
superficial (0 nm)	$\infty$
full water-like cell wall (400 nm)	$0.172\,54\,\text{cm s}^{-1}$
rodlet-melanin layer (10 nm)	$3.43 \times 10^{-5}\,\text{cm s}^{-1}$
rodlet-melanin + agarose-like polysaccharides (200 nm)	$3.43 \times 10^{-5}\,\text{cm s}^{-1}$
rodlet-melanin + agarose-like polysaccharides (400 nm)	$3.429 \times 10^{-5}\,\text{cm s}^{-1}$
rodlet-melanin + cellulose-like polysaccharides (200 nm)	$3.419 \times 10^{-5}\,\text{cm s}^{-1}$
rodlet-melanin + cellulose-like polysaccharides (400 nm)	$3.407 \times 10^{-5}\,\text{cm s}^{-1}$
rodlet-melanin + agarose-like polysaccharides + lipid membrane (203.8 nm)	$2.486 \times 10^{-5}\,\text{cm s}^{-1}$
rodlet-melanin + agarose-like polysaccharides + lipid membrane (403.8 nm)	$2.486 \times 10^{-5}\,\text{cm s}^{-1}$
rodlet-melanin + cellulose-like polysaccharides + lipid membrane (203.8 nm)	$2.481 \times 10^{-5}\,\text{cm s}^{-1}$
rodlet-melanin + cellulose-like polysaccharides + lipid membrane (403.8 nm)	$2.474 \times 10^{-5}\,\text{cm s}^{-1}$

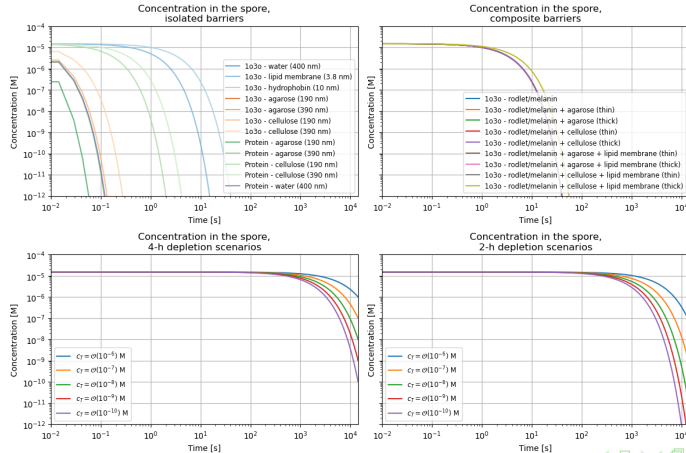
Table: Effective permeability ( $P_{\text{eff}}$ ) of 1-octen-3-ol through different barrier configurations.



# SINGLE-SPORE EXPERIMENTS: REVISION



## Single-spore release scenarios



# SINGLE-SPORE EXPERIMENTS: REVISION



## Single-spore release scenarios

- » The results confirm that, under the assumed initial concentration, the permeation of 1-octen-3-ol and of the hypothetical protein through any of the barrier candidates, isolated or composite, occurs **too fast** to meet any realistic threshold at a time mark longer than 60 seconds.
- » The permeation constants needed for the attainment of the different thresholds are listed in the table below:

$c_T$	$c_0 \times 10^{-1}$	$c_0 \times 10^{-2}$	$c_0 \times 10^{-3}$	$c_0 \times 10^{-4}$	$c_0 \times 10^{-5}$
$P_s(4 \text{ h}) [\text{cm/s}]$	$1.56715868 \times 10^{-8} \text{ cm s}^{-1}$	$2.8996732 \times 10^{-8} \text{ cm s}^{-1}$	$4.23218772 \times 10^{-8} \text{ cm s}^{-1}$	$5.56470225 \times 10^{-8} \text{ cm s}^{-1}$	$6.89721677 \times 10^{-8} \text{ cm s}^{-1}$
$P_s(1 \text{ h}) [\text{cm/s}]$	$3.13431736 \times 10^{-8} \text{ cm s}^{-1}$	$5.7993464 \times 10^{-8} \text{ cm s}^{-1}$	$8.46437545 \times 10^{-8} \text{ cm s}^{-1}$	$1.112940449 \times 10^{-7} \text{ cm s}^{-1}$	$1.379443353 \times 10^{-7} \text{ cm s}^{-1}$

- » The release mechanism possibly involves stronger interaction between the inhibitor and the cell wall.

# SINGLE-SPORE EXPERIMENTS: REVISION



## Single-spore release scenarios

- » In a potential cell wall adsorption model, the permeation constant could be shaped by the Langmuir isotherm equation:

$$P_{\text{eff}} = \frac{P_s}{1 + KB_{\text{max}}}. \quad (2)$$

- » The implications of such a mechanism are yet to be studied.

# OUTLINE



## 1 Single-spore experiments: revision

Introduction

Revision of diffusivities/permeabilities

Barrier scenarios

Table of permeabilities

Single-spore release scenarios

Cell wall adsorption model

## 2 Spore cluster experiments: revision

Introduction

Homogeneous vs. cell-wall-bound inhibitor

Extreme cases

Functional relationship

## 3 From a deterministic to a statistical model

Deriving the germination probability

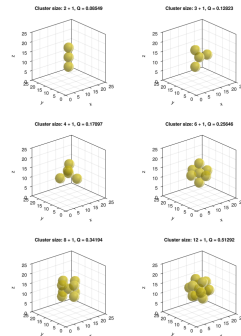
Parameter estimation

# SPORE CLUSTER EXPERIMENTS: REVISION



## Introduction

- » Previously, it was found that neighbour clusters affect diffusivity, but this effect could not be reproduced across all models.
- » An error was found in the high-resolution solver and was corrected.
- » Hence, the cluster simulations were repeated.

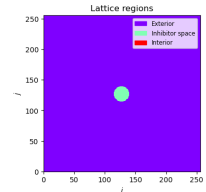
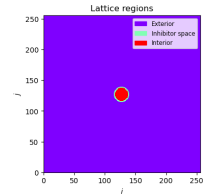
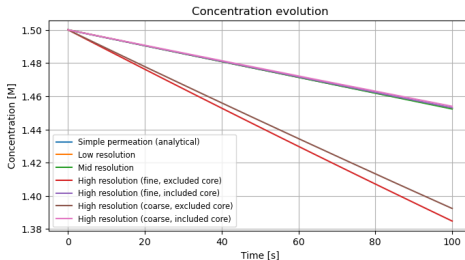


# SPORE CLUSTER EXPERIMENTS: REVISION



## Homogeneous vs. cell-wall-bound inhibitor

- » It was found that, if the inhibitor is **only in the cell wall**, it is released faster compared to a **homogenous distribution** in the spore volume.
- » The reason for this is that there is a higher concentration "pressure" for the same amount of molecules.



# SPORE CLUSTER EXPERIMENTS: REVISION



## Extreme cases

- » The inhibitor release was compared between a **single spore** and a **full cluster of 12+1 spores**.
- » The results show that the neighbours *in direct contact* still obstruct inhibitor release, but to a much lesser degree (7% more residual concentration at  $t = 4$  h).
- » If the inhibitor is only in the cell wall and the spore interiors are inaccessible, the blocking effect is stronger (20% more residual concentration at  $t = 4$  h).

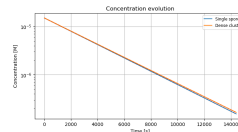


Figure: Empty spore interior.

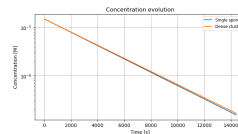


Figure: Full spore interior.

# SPORE CLUSTERS VS. RELEASE EXPONENT



## Functional relationship

- » The neighbour arrangements produce fluctuating results in the measured release exponent.
- » The results are sensitive to the arrangement of neighbours around the central spore (symmetric vs. asymmetric).
- » Finite lattice size with absorbing boundary possibly distorts the results.
- » A fitted power-law yields a relationship  $c(t) \sim e^{\alpha t/\tau}$ , where  $\alpha \sim M^{-0.004}$ , i.e. a very slow decrease with increasing number of neighbours  $M$ .
- » In general, as diffusion through the cluster gaps still depletes the inhibitor locally. Thus, **clustering is not critical in slowing down inhibitor release**.
- » It is to be investigated whether the cluster effect is amplified by the combination of density-driven inhibitor saturation.

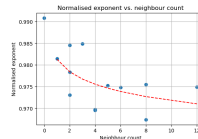


Figure: Empty spore interior.

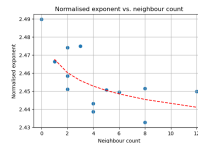


Figure: Full spore interior.



# OUTLINE



## 1 Single-spore experiments: revision

Introduction

Revision of diffusivities/permeabilities

Barrier scenarios

Table of permeabilities

Single-spore release scenarios

Cell wall adsorption model

## 2 Spore cluster experiments: revision

Introduction

Homogeneous vs. cell-wall-bound inhibitor

Extreme cases

Functional relationship

## 3 From a deterministic to a statistical model

Deriving the germination probability

Parameter estimation

# FROM A DETERMINISTIC TO A STATISTICAL MODEL

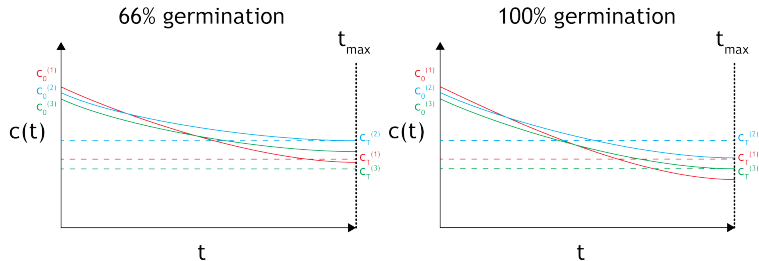


## Deriving the germination probability

- » Spores are heterogeneous. This means that the parameters of the deterministic formula

$$c_{\text{in}}(t) = \phi c_0 + (1 - \phi) \left[ c_{\text{ex}} + (c_0 - c_{\text{ex}}) e^{-\frac{t}{\tau(1-\phi)}} \right], \quad \tau = \frac{V_s}{P_s A}, \quad (3)$$

may vary randomly, with specific distributions.



# FROM A DETERMINISTIC TO A STATISTICAL MODEL



## Deriving the germination probability

- » Each spore is approximately spherical, so the surface-to-volume ratio can be expressed through the **spore radius**  $R$ :  $\frac{V_s}{A} \approx \frac{\frac{4}{3}\pi R^3}{4\pi R} = \frac{R}{3}$ . The radius can be modelled by a **random variable**  $\xi$ .
- » The **spore density** can be considered a **constant**, so the volume fraction  $\phi$  varies only depending on the radius via the spore volume ( $\phi = \rho_s V_s$ ).
- » The **permeation coefficient** is a **constant**.
- » The **initial concentration**  $c_0$  and the **concentration threshold**  $c_T$  for germination inhibition vary **randomly**.

# FROM A DETERMINISTIC TO A STATISTICAL MODEL



## Deriving the germination probability

- » The onset of germination can be observed at slightly varying times, but this randomness can be absorbed by the threshold variable  $c_T$
- » Thus, expressing

$$c_{\text{in}}(t_{\text{germ}}) = \beta c_0, \quad (4)$$

where  $\beta = \phi + (1 - \phi)e^{-\frac{t_{\text{germ}}}{\tau(1-\phi)}}$ , and  $c_T = \gamma c_0$ , where  $\gamma$  is a random variable with an unknown distribution, one can express the condition for germination as

$$\beta c_0 < \gamma c_0, \quad (5)$$

or, simplified,

$$\beta(\xi, \rho_s) < \gamma. \quad (6)$$

# FROM A DETERMINISTIC TO A STATISTICAL MODEL



## Deriving the germination probability

- » When changing the main control parameter of the model, the spore density  $\rho_s$ , the percentage of germinated spores is expressed through the probability

$$p(\rho_s) = P(\beta < \gamma \mid \rho_s). \quad (7)$$

- » Accounting for the distribution of  $\xi$ ,

$$p(\rho_s) = \int_0^\infty P(\beta < \gamma \mid \rho_s, \xi) f_\xi(\xi) d\xi, \quad (8)$$

where  $f_\xi(\xi)$  is the probability distribution function (PDF) for the spore radius. For simplicity, it can be assumed that  $\gamma$  and  $\xi$  are **normally distributed**. Then,

$$P(\beta < \gamma \mid \rho_s, \xi) = 1 - \Phi\left(\frac{\beta(\xi) - \mu_\gamma}{\sigma_\gamma}\right). \quad (9)$$

# FROM A DETERMINISTIC TO A STATISTICAL MODEL



## Deriving the germination probability

- » The PDF of  $\xi$  is then the Gaussian function

$$f_{\xi}(\xi) = \frac{1}{\sqrt{2\pi}\sigma_{\xi}} \exp\left(-\frac{(\xi - \mu_{\xi})^2}{2\sigma_{\xi}^2}\right). \quad (10)$$

- » Thus, the germination probability can be expressed as

$$p(\rho_s) = \int_0^{\infty} \left[1 - \Phi\left(\frac{\beta(\xi) - \mu_{\gamma}}{\sigma_{\gamma}}\right)\right] \frac{1}{\sqrt{2\pi}\sigma_{\xi}} \exp\left(-\frac{(\xi - \mu_{\xi})^2}{2\sigma_{\xi}^2}\right) d\xi. \quad (11)$$

- » The mean and standard deviation of the spore radius can be inferred from literature. For instance, the diameter of *A. niger* is 5.3(6)  $\mu\text{m}$  ( $\mu_{\xi} = 2.65 \mu\text{m}$  and  $\sigma_{\xi} = 0.3 \mu\text{m}$  [3], while the diameter of *A. nidulans* is observed to vary between 2.4 and 2.7  $\mu\text{m}$  [5] ( $\mu_{\xi} = 1.275 \mu\text{m}$  and  $\sigma_{\xi} = 0.075 \mu\text{m}$ ).

# FROM A DETERMINISTIC TO A STATISTICAL MODEL



## Deriving the germination probability

- » If an inhibitor concentration is **exogenously added**, the germination condition is

$$\beta c_0 + \chi c_{\text{ex}} < \gamma c_0 \quad (12)$$

- »  $c_0$  does not cancel, can be modelled by a random variable  $\psi$ . The probability formula becomes

$$p(\rho_s, c_{\text{ex}}) = \int_0^\infty \int_0^\infty \left[ 1 - \Phi \left( \frac{\beta(\xi) + \chi \frac{c_{\text{ex}}}{\psi} - \mu_\gamma}{\sigma_\gamma} \right) \right] f_\psi(\psi) f_\xi(\xi) d\psi d\xi, \quad (13)$$

where the two PDFs are

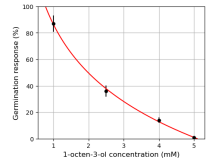
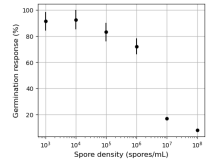
$$f_\psi(\psi) = \frac{1}{\sqrt{2\pi}\sigma_\psi} e^{-\frac{(\psi - \mu_\psi)^2}{2\sigma_\psi^2}}, \quad f_\xi(\xi) = \frac{1}{\sqrt{2\pi}\sigma_\xi} e^{-\frac{(\xi - \mu_\xi)^2}{2\sigma_\xi^2}}. \quad (14)$$

# FROM A DETERMINISTIC TO A STATISTICAL MODEL



## Parameter estimation

- » Using the probability formula, the unknown parameters  $P_s$ ,  $\mu_\gamma$  and  $\sigma_\gamma$  are fit on data by Herrero-Garcia et al. [2], including
  - germination response under varying spore density,
  - germination response under added concentrations of 1-octen-3-ol.
- » The fitting process aims to investigate whether
  - the inhibition effects of spore density and added 1-octen-3-ol have the same underlying mechanism,
  - the model can capture both of these effects.





# FROM A DETERMINISTIC TO A STATISTICAL MODEL



## Parameter estimation

- » Fitting the model to the density-driven germination data only, the transition in germination rates around  $10^5$  spores/mL is captured.

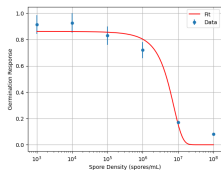


Figure: Model fitted to density-driven germination data.

- » Fixing the  $P_s$ ,  $\mu_\gamma$  and  $\sigma_\gamma$  from the last fit,  $\mu_\psi$  and  $\sigma_\psi$  are fit again under varying  $c_{ex}$ . The match is unsatisfactory.

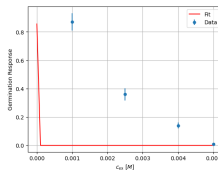


Figure: Model fitted to exogenously driven germination data.

- » Fitting  $P_s$ ,  $\mu_\gamma$ ,  $\sigma_\gamma$ ,  $\mu_\psi$  and  $\sigma_\psi$  on both models does not produce a good match.

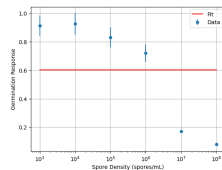


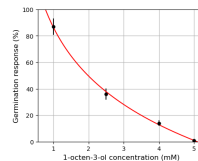
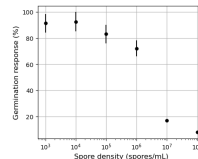
Figure: Model fitted to both data simultaneously.

# FROM A DETERMINISTIC TO A STATISTICAL MODEL



## Parameter estimation

- » The model can represent density-driven inhibition somewhat accurately (under  $c_{ex} = 0$ ).
- » The model cannot represent both density-driven inhibition and exogenously driven inhibition simultaneously.
- » The mechanisms behind the two phenomena may indeed be different:
  - It is known that the thresholds for exogenous inhibition are higher than the presumed spore concentration [4],
  - so 1-octen-3-ol likely does not act alone.

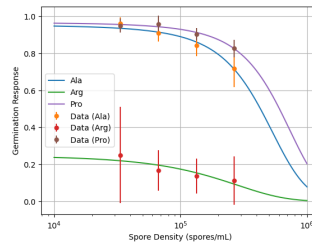


# FROM A DETERMINISTIC TO A STATISTICAL MODEL



## Parameter estimation

- » The parameters  $P_s$ ,  $\mu_\gamma$  and  $\sigma_\gamma$  are fit again on data by Ijadpanahsaravi et al. [3], including density-driven germination rates under different carbon sources.
- » The time-frame is set to 100 hours, since  $P_{\max}$  is a long-time asymptotic limit.
- » The results are consistent with
  - **conserved permeability** - rate of inhibitor release not altered by environmental changes;
  - **varying inhibition threshold** across the different environmental scenarios - carbon signals modulate the inhibition threshold in the spore culture.



Case	$P_s$ [cm s <sup>-1</sup> ]	$\mu_\gamma$	$\sigma_\gamma$
Ala	$3.176 \times 10^{-9}$ cm s <sup>-1</sup>	$3.780 \times 10^{-5}$	$1.819 \times 10^{-5}$
Arg	$2.741 \times 10^{-9}$ cm s <sup>-1</sup>	$1.000 \times 10^{-10}$	$2.213 \times 10^{-5}$
Pro	$3.109 \times 10^{-9}$ cm s <sup>-1</sup>	$5.284 \times 10^{-5}$	$2.345 \times 10^{-5}$



- [1] Birger Brodin, Bente Steffansen, and Carsten Uhd Nielsen. "Passive diffusion of drug substances: the concepts of flux and permeability". In: *Molecular Biopharmaceutics*. 2010. URL: <https://api.semanticscholar.org/CorpusID:12995364>.
- [2] Erika Herrero-García et al. "8-Carbon oxylipins inhibit germination and growth, and stimulate aerial conidiation in *Aspergillus nidulans*". In: *Fungal biology* 115 4-5 (2011), pp. 393–400. URL: <https://api.semanticscholar.org/CorpusID:33687383>.
- [3] Maryam Ijadpanahsaravi et al. "The impact of inter- and intra-species spore density on germination of the food spoilage fungus *Aspergillus niger*". In: *International journal of food microbiology* 410 (2023), p. 110495. URL: <https://api.semanticscholar.org/CorpusID:265268197>.
- [4] Kana Miyamoto et al. "Formation of 1-octen-3-ol from *Aspergillus flavus* conidia is accelerated after disruption of cells independently of Ppo oxygenases, and is not a main cause of inhibition of germination". In: *PeerJ* 2 (2014). URL: <https://api.semanticscholar.org/CorpusID:8514039>.



- [5] Jae-Hyuk Yu. "Regulation of Development in *Aspergillus nidulans* and *Aspergillus fumigatus*". In: *Mycobiology* 38 (2010), pp. 229 -237. URL: <https://api.semanticscholar.org/CorpusID:17713460>.